Mössbauer studies of the static and dynamic critical behavior of the layered antiferromagnets $RbFeF_4$ and $KFeF_4$

Hugo Keller and Ilija M. Savić*
Physik-Institut, Universität Zürich, CH-8001 Zürich, Switzerland
(Received 8 February 1983)

Detailed ^{57}Fe Mössbauer studies of the static and dynamic critical behavior of the layered antiferromagnets $RbFeF_4$ and $KFeF_4$ are reported. All measurements were performed on single crystals with the direction of the γ rays perpendicular to the magnetic layers. Both systems undergo a second-order phase transition at the Néel temperature $T_N=133.57(2)$ K for $RbFeF_4$ and $T_N=135.79(2)$ K for $KFeF_4$. Special attention was given to a careful evaluation of reliable values for the critical indices. In the asymptotic critical region below T_N, the temperature dependence of the hyperfine field H is well described by the power law $H \propto t^{\beta}$, where β is the static critical exponent of the order parameter, and $t=1-T/T_N$ is the reduced temperature. The following asymptotic values for β were found: $\beta=0.316(3)$ for $RbFeF_4$ in the range $5\times10^{-4}<t<10^{-2}$ and $\beta=0.151(3)$ for $KFeF_4$ in the range $3.8\times10^{-4}<t<5.7\times10^{-2}$. These results indicate that $RbFeF_4$ shows a three-dimensional critical behavior, in contrast to $KFeF_4$, where the magnetic transition is essentially two dimensional in nature. The present values for β disagree considerably with the nonasymptotic values previously reported by other groups. Just above T_N a characteristic line broadening $\Delta\Gamma$ due to critical spin fluctuations is observed. At the critical point $\Delta\Gamma$ diverges as $\Delta\Gamma \propto |t|^{-w}$, where the exponent w involves, besides two static exponents, the dynamic exponent z. In the critical region $10^{-4}<|t|<10^{-3}$, the following values for w and the corresponding values for z were obtained: $w=0.81(6)$, $z=2.15(19)$ for $RbFeF_4$ and $w=0.91(5)$, $z=1.29(9)$ for $KFeF_4$. These values are compared to those predicted by the current theory of critical dynamics. At T_N the center shift and the quadrupole splitting show a pronounced anomaly that appears to be associated with the onset of magnetic ordering.

I. INTRODUCTION

Over the past few years there has been great interest in experimental work on critical phenomena with special emphasis on simple magnetic systems[1] with effective lattice dimensionality $d=1$, 2, and 3. A fundamental question of interest is to what extent such experiments support theoretical predictions and how far they may contribute to a deeper understanding of critical phenomena in simple systems. However, such experiments demand exceptional care to guarantee deduction of reliable critical indices. In order to avoid erroneous results, the following precautions should be taken into account: (i) The data should be taken very close to the critical point T_C. (ii) The asymptotic critical region must be determined experimentally in each case.[2] (iii) Temperature instabilities, temperature gradients, sample inhomogeneities, and mechanical stress on the sample should be avoided. Unfortunately, these important facts have been neglected by many experimentalists. For example, a large percentage of the earlier experimental results[1] are found to be not sufficiently conclusive to allow a direct comparison with theoretical predictions.

Precise and comprehensive Mössbauer work on critical phenomena in three-dimensional (3D) Heisenberg ferromagnets has been conducted by Hohenemser and his collaborators (see references). A critical review of measurements of the critical exponent β in 3D magnetic systems has been given by Suter and Hohenemser[2] who have reanalyzed experimental data for various 3D compounds. As a result they have found that the number of accurate values of β available in the literature is small. A detailed Mössbauer study of the static and dynamic critical behavior in iron has been recently published by Kobeissi.[3] However, not much Mössbauer work has been done on critical phenomena in quasi-two-dimensional (2D) magnetic systems, especially, on critical spin dynamics, where only a limited number of experimental results have been reported.

The static critical behavior of the layered antiferromagnets of the form $XFeF_4$ (X=Rb,K,Cs) has been studied by several authors.[4–8] However, none of the reported values of the critical exponent β is in agreement with theoretical predictions for either a 2D magnetic system or a 3D magnetic system. The reason for this discrepancy, as we will demonstrate in this paper, is the fact that these values for β were determined outside the appropriate critical region.

In this work we present detailed ^{57}Fe Mössbauer studies of the static and dynamic critical behavior of single crystals of $RbFeF_4$ and $KFeF_4$. In contrast to previous results,[4–8] we find that $RbFeF_4$ shows a 3D critical behavior, whereas in $KFeF_4$ the magnetic phase transition is essentially 2D in nature. Furthermore, in both systems the center shift and the quadrupole splitting display an anomalous behavior near the critical temperature that appears to be induced by the onset of magnetic ordering.

The organization of this paper is as follows. In Sec. II

we briefly review the principal features of the theory of critical phenomena, insofar as is relevant to the analysis and interpretation of our measurements. A general discussion of the magnetic properties of layered magnetic systems, together with the crystallographic and magnetic structures of $RbFeF_4$ and $KFeF_4$ is given in Sec. III. Experimental details and preliminary results such as the interpretation of Mössbauer spectra and the deduced hyperfine parameters are presented in Sec. IV. In Sec. V we discuss the experimental results of the static and dynamic critical behavior of $RbFeF_4$ and $KFeF_4$, as well as possible reasons for the critical anomalies in the center shift and the quadrupole splitting observed near the transition temperature. The conclusions follow in Sec. VI.

II. THEORY OF CRITICAL BEHAVIOR

When the temperature of a magnetic system approaches the critical temperature T_C, anomalies occur in the static and dynamic properties. These anomalies have been characterized in terms of critical exponents. Static properties are thermodynamic quantities which are determined by the equilibrium distribution of the spins at a given instant in time. According to the static universality hypothesis,[9] the static exponents of a system with short-range interaction depend primarily on the lattice dimensionality d and the dimension n of the order parameter, but not on the details of the interaction. The dynamic properties, on the other hand, are quantities such as relaxation rates and transport coefficients, which are determined by the equations of motion. The critical dynamics therefore depend, in addition, on conservation laws which do not affect the static behavior.[10]

A. Static behavior ($T < T_C$)

The static critical behavior of the order parameter (spontaneous magnetization) $M(T)$ of a magnetic system is characterized by the critical exponent β which is defined by the asymptotic relation[9]

$$\sigma(t)=Bt^{\beta}\ , \quad t\to 0 \tag{1}$$

where $\sigma(t)=M(T)/M(0)$ is the reduced magnetization, t is the reduced temperature, $t=1-T/T_C$, and B is a numerical constant which depends only on lattice symmetry and spin value. For temperatures not sufficiently close to T_C, Eq. (1) must be modified with a correction-to-scaling term[11,12]

$$\sigma(t)=Bt^{\beta}[1+At^{\tilde{\Delta}}+O(t^{2\tilde{\Delta}})]\ , \tag{2}$$

where A is the correction-to-scaling amplitude and $\tilde{\Delta}$ is the correction-to-scaling exponent. The exponent $\tilde{\Delta}$ is universal, whereas the amplitude A depends on the system. However, recently it has been shown that the ratios among the correction-to-scaling amplitudes for any two exponents are universal.[12,13] Experimental data which are fitted with a pure power law $\sigma(t)\simeq B^*t^{\beta^*}$ will yield an effective exponent β^* that is related to the universal β by[11,12]

$$\beta^*=\beta+A\tilde{\Delta}t^{\tilde{\Delta}}+O(t^{2\tilde{\Delta}})\ , \quad \lim_{t\to 0}\beta^*=\beta\ . \tag{3}$$

This means for $t\to 0$, β^* depends on the nonuniversal correction-to-scaling amplitude A and on the reduced temperature t. From an experimental point of view, it is important to note that effective exponents also obey all the scaling relations (e.g., $\alpha^*+2\beta^*+\gamma^*=2$), except those of hyperscaling.[11,12] Precise numerical values for β and $\tilde{\Delta}$ for 3D systems have been obtained by renormalization-group methods.[14] These values together with the exact results for the 2D Ising model are summarized in Table I.

Mössbauer spectroscopy is a very sensitive method to study critical phenomena in magnetic solids.[15] Measurements of the hyperfine field $H(T)$ are used to probe the spontaneous magnetization (sublattice magnetization) $M(T)$ in a ferromagnet (antiferromagnet). It is generally assumed that $H(T)$ is proportional to $M(T)$. This is not a trivial relation,[16] because the reduced magnetization σ may deviate from the reduced hyperfine field $h=H(T)/H(0)$ well below T_C. However, in our case of an Fe^{3+} ion ($^6S_{5/2}$), this is a rather good approximation.[7] Thus we may write Eq. (1) as[16,17]

$$h(t)=\sigma(t)=Bt^{\beta}\ , \quad t\to 0\ . \tag{4}$$

B. Critical dynamics ($T > T_C$)

Far above T_C atomic spins fluctuate with frequencies which are too high to be observed by a Mössbauer experiment. However, as T approaches T_C, clusters of correlated spins form, and thus the motion of individual spins slows down. These clusters are defined in space and time in terms of the correlation length ξ and the characteristic lifetime τ_0. At T_C, where the system orders, both quantities ξ and τ_0 diverge, and the characteristic frequency of the spin fluctuations ω_c goes to zero (critical slowing down). This phenomenon may be observed under certain conditions by a hyperfine-interaction experiment.[15,18,19]

In theoretical treatments of critical spin fluctuations one considers the space-time spin correlation function defined by

$$G^{\alpha\alpha}(\vec{r},t)=\langle S^{\alpha}(\vec{r},t)S^{\alpha}(0,0)\rangle\ , \quad \alpha=x,y,z\ . \tag{5}$$

A more convenient physical quantity than $G^{\alpha\alpha}(\vec{r},t)$ itself is the dynamic structure factor $S^{\alpha\alpha}(\vec{k},\omega)$, which is the space-time Fourier transform of $G^{\alpha\alpha}(\vec{r},t)$. In the following we adopt the formulation of critical dynamics as described in detail in the review of Hohenberg and Halperin.[10] In this theory the dynamic correlation function

TABLE I. Critical exponent β and correction-to-scaling exponent $\tilde{\Delta}$ for various static universality classes (d,n).

	n	β	$\tilde{\Delta}$
$d=2$			
Ising	1	0.125	1
$d=3$[a]			
Ising	1	0.325(1)	0.493(7)
XY	2	0.346(1)	0.521(6)
Heisenberg	3	0.365(1)	0.550(5)

[a]Le Guillou and Zinn-Justin, Ref. 14.

$S^{\alpha\alpha}(\vec{k},\omega)$ is written in the general form

$$S^{\alpha\alpha}(\vec{k},\omega)=2\pi[\omega_c^{\alpha\alpha}(\vec{k})]^{-1}S^{\alpha\alpha}(\vec{k})f_{k\xi}(\omega/\omega_c^{\alpha\alpha}(\vec{k}))\ , \tag{6}$$

where $\omega_c^{\alpha\alpha}(\vec{k})$ is the characteristic frequency of the fluctuations with wave vector $\vec{k}$, $S^{\alpha\alpha}(\vec{k})$ is the static structure factor, and $f_{k\xi}(\omega/\omega_c^{\alpha\alpha}(\vec{k}))$ is the shape function of the energy line. According to static and dynamic scaling hypotheses,[10] $S^{\alpha\alpha}(\vec{k})$ and $\omega_c^{\alpha\alpha}(\vec{k})$ are homogeneous functions of k and ξ^{-1}:

$$S^{\alpha\alpha}(\vec{k})=k^{-2+\eta}g^{\alpha\alpha}(k\xi)\ , \tag{7}$$

$$\omega_c^{\alpha\alpha}(\vec{k})=k^z\Omega^{\alpha\alpha}(k\xi)=\xi^{-z}\Omega_*^{\alpha\alpha}(k\xi)\ . \tag{8}$$

Here $g^{\alpha\alpha}(k\xi)$, $\Omega^{\alpha\alpha}(k\xi)$, and $\Omega_*^{\alpha\alpha}(k\xi)$ are scaling functions, η is the universal static exponent, and z is the dynamic exponent. The temperature dependence of Eqs. (6)–(8) stems from that of the correlation length ξ which at T_C diverges as

$$\xi\propto t^{-\nu}\ , \tag{9}$$

where $t=T/T_C-1$ is the reduced temperature, and ν is the universal static exponent. As a consequence Eqs. (8) and (9) imply that the characteristic frequency $\omega_c^{\alpha\alpha}(\vec{k})$ of the critical fluctuations with wave vector $\vec{k}$ goes to zero as $\omega_c^{\alpha\alpha}(\vec{k})\propto t^{\nu z}$ for $t\to 0$ (critical slowing down).

In a Mössbauer experiment one measures the spin-autocorrelation time τ_c^α defined by the time integral[15]

$$\tau_c^\alpha=\tfrac{1}{2}\int_{-\infty}^{+\infty}[G^{\alpha\alpha}(0,t)/G^{\alpha\alpha}(0,0)]dt\ . \tag{10}$$

This expression is easily written in terms of $S^{\alpha\alpha}(\vec{k},\omega)$:

$$\tau_c^\alpha\propto\int_{V_k}d^dk\,S^{\alpha\alpha}(\vec{k},\omega=0)\ , \tag{11}$$

where V_k is the Brillouin-zone volume. The evaluation of this integral is straightforward. Using the scaling form of $S^{\alpha\alpha}(\vec{k},\omega=0)$ defined by Eqs. (6)–(8), one finds[19,20]

$$\tau_c^\alpha\propto\xi^{z+2-d-\eta}\propto t^{-w}\ , \tag{12a}$$

$$w=\nu(z+2-d-\eta)\ . \tag{12b}$$

In an experiment, w is determined directly by a measurement of τ_c^α for $T\to T_C$, and with the knowledge of the static exponents η and ν, the dynamic exponent z may be extracted from the measured w. For the present work it is convenient to express w in terms of other static exponents, such as β, γ, and ν. This is easily done by using the static scaling relations[9]

$$z=\frac{d}{\gamma+2\beta}(w+2\beta)=\frac{1}{\nu}(w+2\beta)\ . \tag{13}$$

According to the current theory,[9] the static exponents are universal within a class of systems belonging to the same static universality class (d,n). The dynamic exponent z, on the other hand, depends, in addition, on conservation laws satisfied by the Hamiltonian.[10] Theoretical values of the exponents z and w for antiferromagnetic systems belonging to different dynamic universality classes are listed in Table II. A discussion of this table follows in Sec. V B.

In a Mössbauer experiment critical spin fluctuations induce corresponding fluctuations in the hyperfine field, giving rise to a line broadening $\Delta\Gamma$ of the Mössbauer line:

$$\Gamma=\Gamma_0+\Delta\Gamma\ , \tag{14}$$

where Γ and Γ_0 are the observed and natural linewidth [full width at half maximum (FWHM)], respectively. In order to relate $\Delta\Gamma$ to the spin-autocorrelation time τ_c^α, an appropriate relaxation theory is needed.[15] Here, we adopt the theory of Bradford and Marshall[22] who have used perturbation theory to calculate the ^{57}Fe Mössbauer line shape in the limit of fast electronic relaxation. In the case of an isotropic hyperfine interaction there is one correlation time $\tau_c=\tau_c^\alpha$ $(\alpha=x,y,z)$. For a single-crystal absorber with the principal axis of the uniaxial electric field gradient tensor parallel to γ direction (cf. Sec. IV B), the relaxation spectrum consists of two asymmetric Lorentzians[22]:

$$A(\omega)\sim\frac{(\Gamma_0/2)+C_1\tau_c}{[\omega-(\Delta/2)]^2+[(\Gamma_0/2)+C_1\tau_c]^2}+\frac{1}{3}\frac{(\Gamma_0/2)+C_2\tau_c}{[\omega+(\Delta/2)]^2+[(\Gamma_0/2)+C_2\tau_c]^2}\ , \tag{15}$$

with

TABLE II. Dynamic exponent z and exponent w for antiferromagnetic systems as predicted by current theory [after Hohenberg and Halperin (Ref. 10)].

Dynamical model[a]	Static universality class (d,n)	z[b]	$w=\nu(z+2-d-\eta)$[b]
Conventional theory	(3,1)	$2-\eta=1.968$	0.590
Model A (anisotropic)	(3,1)	$2-\eta+z'=1.993$[c]	0.606
Model C (anisotropic)	(3,1)	$2+\alpha/\nu=2.174$	0.720
Model G (isotropic)	(3,3)	$d/2=1.5$	0.329
Conventional theory	(2,1)	$2-\eta=1.75$	1.5
Model A (anisotropic)	(2,1)	1.4–2.2[d]	1.15–1.95
Model G (isotropic)	(2,3)	$d/2=1$	

[a]The meaning of the models (A,C,G) is explained in Ref. 10.
[b]Numerical values for the 3D static exponents are taken from Ref. 14.
[c]The exponent z' is defined in Ref. 21.
[d]Reference 21.

$$C_1=\frac{S(S+1)}{3\hbar^2}(\tfrac{3}{4}A_g^2-\tfrac{3}{2}A_gA_e-\tfrac{3}{4}A_e^2)$$

and

$$C_2=\frac{S(S+1)}{3\hbar^2}(\tfrac{3}{4}A_g^2+\tfrac{1}{2}A_gA_e+\tfrac{15}{4}A_e^2)\ , \tag{16}$$

where A_g and A_e are the hyperfine coupling constants of the ground state and the excited state, respectively, and Δ is the quadrupole splitting. Note that C_1 and C_2 are roughly the same for ^{57}Fe. Equation (15) is only valid if the following assumptions are made: (i) The fluctuations are isotropic. (ii) The correlation function $G(\vec{r},t)$ is exponential.[23] (iii) The inequalities $\tau_c\omega_L \ll 1$, $\tau_c^2\Delta^2 \ll 1$, $\tau_c\Delta\Gamma \ll 1$, and $\Delta\Gamma/\omega_L \ll 1$ hold, where ω_L is the nuclear Larmor frequency. All these inequalities are fulfilled for the cases investigated in this paper. Furthermore, we assume that the fluctuations are isotropic. This is of course not a trivial assumption as in our case of a weakly anisotropic Heisenberg system (cf. Sec. II). From Eqs. (12) and (15), it follows that for $t\rightarrow 0$ the average excess linewidth $\Delta\Gamma$ (FWHM) of the two quadrupole lines diverges as

$$\Delta\Gamma=(C_1+C_2)\tau_c=Dt^{-w}\ , \tag{17}$$

where D is a numerical constant.

In contrast to neutron scattering,[18,19] the Mössbauer effect probes an integral property of the dynamic structure factor $S^{\alpha\alpha}(\vec{k},0)$ [Eq. (11)]. As $T\rightarrow T_C$, $S^{\alpha\alpha}(\vec{k},\omega)$ becomes a sharp peak near $k=0$. Thus the integrand in Eq. (11) is mainly weighted by small k values[19] that are usually only accessible in a high-resolution neutron scattering experiment. The Mössbauer effect therefore offers an alternative method to study critical spin dynamics in magnetic systems in the limit $T\rightarrow T_C$.

III. LAYERED MAGNETIC SYSTEMS

A weakly anisotropic Heisenberg system consisting of coupled antiferromagnetic layers of localized spins $\vec{S}$ may be described by the Hamiltonian[24]

$$\mathcal{H}=-2J\sum_{\langle ij\rangle}^{xy}\vec{S}_i\cdot\vec{S}_j-2J'\sum_{\langle ij\rangle}^{z}\vec{S}_i\cdot\vec{S}_j-g\mu_B\sum_i^{xyz}H_A^iS_i^z\ , \tag{18}$$

where J and J' are the intralayer and interlayer exchange interactions, respectively, and H_A^i is an internal staggered anisotropic field which aligns the spins along the z axis. For a system of quasi-isolated magnetic layers $|J'/J| \ll 1$. Mermin and Wagner[25] have proved rigorously that the ideal 2D isotropic Heisenberg system cannot be ordered at nonzero temperatures. However, Stanley and Kaplan[26] have shown that a new kind of phase transition to a state with infinite magnetic susceptibility, but no long-range order, exists if the spin-correlation function [Eq. (5)] in two dimensions decreases with spin separation r more slowly than r^{-2}. The corresponding transition temperature T_{SK} (Stanley-Kaplan temperature) is given within a few percent by[26]

$$T_{SK}\simeq\tfrac{1}{5}(z-1)[2S(S+1)-1]J/k_B\ ,\quad S>\tfrac{1}{2}\ , \tag{19}$$

where z is the coordination number in the plane.

Experimentally, such quasi-two-dimensional systems have been found whose long-range ordering occurs at temperatures which agree rather well with the Stanley-Kaplan temperature T_{SK}.[1] In fact, any deviation from the ideal isotropic 2D system such as a small anisotropy and/or interlayer exchange, or even a finite sample size, favors the occurrence of long-range order within the magnetic layers at nonzero temperatures. The transition temperature T_C of a system of weakly coupled magnetic layers is expected to be very close to the Stanley-Kaplan temperature T_{SK} if the anisotropic field H_A and the interlayer exchange field H_E' are much smaller than the intralayer exchange field H_E. Lines[27] has shown that $T_C\approx T_{SK}$ if both $\alpha=H_A/H_E$ and $|J'/J|$ are of the order 10^{-4} to 10^{-3}. Thus experimental values of T_C are expected to be shifted upwards with respect to T_{SK} with increasing anisotropy α and/or relative coupling strength $|J'/J|$. Here one should also note the work of Binder and Landau[28] who have studied the 2D anisotropic Heisenberg model with α varying from 0.005 to 1 ($\alpha=0$, Heisenberg; $\alpha=1$, Ising) using a Monte Carlo technique. Whether the order parameter of a system of weakly coupled magnetic layers shows a 2D Ising-type ($\beta\simeq\frac{1}{8}$) or a 3D ($\beta\simeq\frac{1}{3}$) critical behavior depends on the relative strength of the anisotropy energy $g\mu_BH_A$ and the interlayer exchange J'. If $g\mu_BH_A \gg |J'|$, a 2D Ising-type critical behavior is expected. However, when T_C is approached closely enough, the interlayer coupling J' may become important, and thus the phase transition will be governed by the true 3D properties of the system (lattice dimensionality crossover).[1,24]

In the following section the crystallographic and magnetic structures of the two layered antiferromagnets $RbFeF_4$ and $KFeF_4$ investigated in this paper are discussed. For comparison, various relevant magnetic parameters, defined and discussed in the text, are summarized in Table III. X-ray diffraction studies[29–32] have shown that the crystal structure of both antiferromagnets is orthorhombic. The magnetic Fe^{3+} ($S=\frac{5}{2}$) ions are in the center of slightly tilted and distorted FeF_6 octahedra, forming sheets of magnetic layers that are separated by nonmagnetic layers of Rb^+ and K^+ ions, respectively. The idealized crystallographic structures without distortion and tilting are shown in Fig. 1. It is known from neutron scattering experiments[5,6] that in the ordered state the magnetic moments in both systems are aligned along

TABLE III. Summary of various magnetic parameters for $RbFeF_4$ and $KFeF_4$. The parameters are defined in the text.

Parameter	$RbFeF_4$	$KFeF_4$
T_N (K)	133.57(2)	135.79(2)
J/k_B (K)	$-11.3(9)$[a]	$-13.3(8)$[a]
α	$6.5(5)\times10^{-3}$ [a]	$5.0(5)\times10^{-3}$ [a]
$\lvert J'/J\rvert$	$\simeq10^{-3}$–10^{-2} [b]	$\simeq10^{-4}$ [b]
T_N/T_{SK}	1.19	1.03
T_N/Θ_{CW}	0.51	0.44
Δ_0	0.163[a]	0.167[a]

[a]From Ref. 7.
[b]From Ref. 1.

the c axis. This is in agreement with previous and the present Mössbauer results.[4–8,17,33] The coupling J within the layers is antiferromagnetic and is roughly the same for both compounds (Table III). However, there is an essential difference between the two compounds concerning the magnetic interaction between the layers. In contrast to $RbFeF_4$, the adjacent magnetic layers in $KFeF_4$ are shifted half a lattice constant with respect to each other[6,32] leading to a "staggered" magnetic structure (Fig. 1). Since the interaction within the layers is antiferromagnetic this configuration causes a cancellation of the magnetic interaction between neighboring layers. Consequently, the interaction can take place only via the next-nearest planes, leading to a much weaker interlayer interaction than for $RbFeF_4$. In fact, the ratio of exchange couplings $|J'/J|$ is about 10—100 times smaller for $KFeF_4$ than for $RbFeF_4$ (Table III). The interlayer coupling in $RbFeF_4$ is purely antiferromagnetic,[5] whereas ferromagnetic as well as antiferromagnetic coupling between second-neighbor layers has been observed in $KFeF_4$ by Heger and Geller.[6] They conclude that this is most likely due to a magnetic domain structure present in the sample. An inspection of Table III shows that the intralayer exchange interactions for both compounds are only weakly anisotropic, $\alpha \simeq 5 \times 10^{-3}$, which is typical for layered antiferromagnets with magnetic Fe^{3+} or Mn^{2+} ions ($^6S_{5/2}$).[1] The experimental transition temperature T_N for $KFeF_4$ is very close to the corresponding Stanley-Kaplan temperature T_{SK} [Eq. (19)], whereas for $RbFeF_4$ the experimental T_N is about 20% higher than T_{SK} due to the stronger coupling between neighboring layers. In addition, T_{SK} may be compared to the Curie-Weiss temperature[1]

$$\Theta_{CW} = \tfrac{2}{3} z S(S+1) J/k_B \ . \tag{20}$$

For $z=4$ and $S=\frac{5}{2}$ it follows that $T_{SK}/\Theta_{CW} \simeq 0.42$. This theoretical value is to be compared with the experimental values T_N/Θ_{CW} for $RbFeF_4$ and $KFeF_4$ listed in Table III. All these factors seem to indicate that $KFeF_4$ is a better candidate for a quasi-2D magnetic system than $RbFeF_4$. Indeed, previous neutron scattering studies of Heger and Geller[6] show evidence for a 2D nature of magnetic ordering in $KFeF_4$ near T_N. The experimental data presented in this paper strongly corroborate this conjecture (cf. Sec. V).

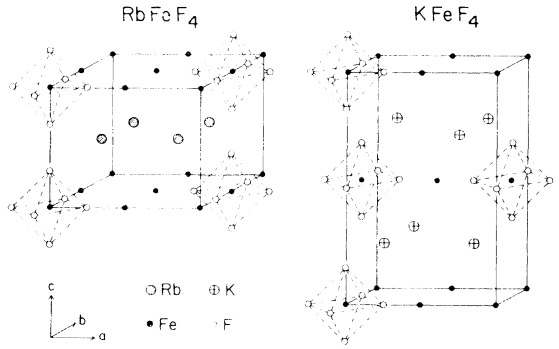

FIG. 1. Idealized crystal structures of $RbFeF_4$ and $KFeF_4$. For clarity only a few FeF_6 octahedra are shown, without distortion and tilting.

IV. EXPERIMENTAL DETAILS AND RESULTS

A. Experimental details

All Mössbauer measurements were performed with single-crystal samples of $RbFeF_4$ and $KFeF_4$ with the γ direction perpendicular to the magnetic layers. Single-crystal samples were used with typical areas of 20 mm^2 and rather large effective thickness (about 7 mg Fe/cm^2). The samples were mounted in vacuum-tight Plexiglas holders surrounded with a thin foil of pure aluminum to guarantee good temperature stability and homogeneity in the sample. Measurements above 80 K were taken in a cold-finger cryostat with a silicon diode temperature sensor (Lake Shore Cryotronics, Inc.). A four-point method, with an accurate 10-μA constant-current source and a high-precision reference voltage, was used to measure and stabilize the sample temperature. The temperature control unit was itself temperature stabilized to better than ± 0.2 K. During the measurements the sample temperature was recorded constantly on a chart recorder. With this arrangement, a relative long-term temperature stability (24 h) of better than ± 5 mK was obtained. Below 80 K, the measurements were performed in a continuous-flow helium cryostat. In this case the sample temperature was stabilized to better than ± 0.1 K with the use of the same type of silicon diode sensor. The absolute temperature accuracy was estimated to be ± 0.5 K for all measurements. The spectra were taken with a conventional constant acceleration spectrometer with a 25-mCi ^{57}CoRh source. The velocity scale was calibrated with a laser interferometer and standard absorbers. Even after several cooling cycles the same spectra within errors were obtained.

B. Results

Typical single-crystal spectra of $RbFeF_4$ and $KFeF_4$ at various temperatures are shown in Figs. 2–4. In all figures the solid lines correspond to best fits through the data points. Above the Néel temperature T_N the spectra show pure asymmetric quadrupole lines. In the antiferromagnetic phase, complex spectra with mixed electric quadrupole and magnetic dipole interactions are observed. These spectra were analyzed using a Hamiltonian fitting procedure[34] that includes self-absorption corrections for thick crystals. The corresponding least-squares fits yield the following parameters: the hyperfine field H, the quadrupole splitting Δ, the center shift δ (relative to metallic iron), the linewidth Γ (FWHM), the asymmetry parameter η of the electric-field-gradient tensor (EFG), the polar angle θ of H in the EFG principal-axis system, and the angle θ_γ between the wave vector $\vec{k}$ of the γ ray and the principal axis V_{zz} of the EFG tensor. The paramagnetic spectra were analyzed with two Lorentzians taking self-absorption into account. Parts of our results are already published in a short form.[17,35] Some relevant Mössbauer parameters obtained for $RbFeF_4$ and $KFeF_4$ are summarized in Table IV. The hyperfine parameters of the two compounds are very similar and are essentially in agreement with earlier measurements.[5–8,33] The angle θ_γ between the principal component V_{zz} of the axially symmetric EFG tensor

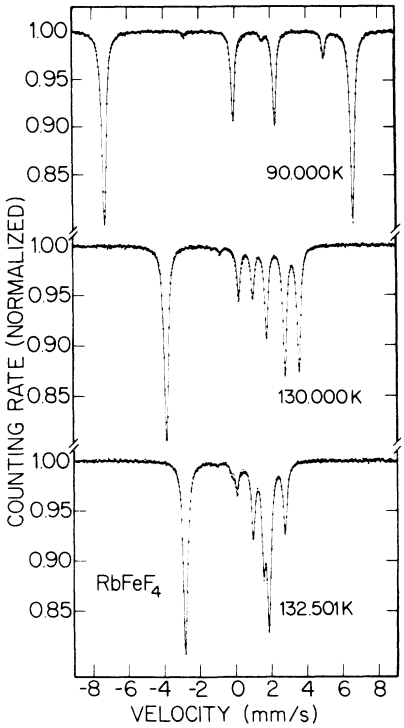

FIG. 2. Mössbauer spectra of single-crystal $RbFeF_4$ taken at various temperatures below T_N.

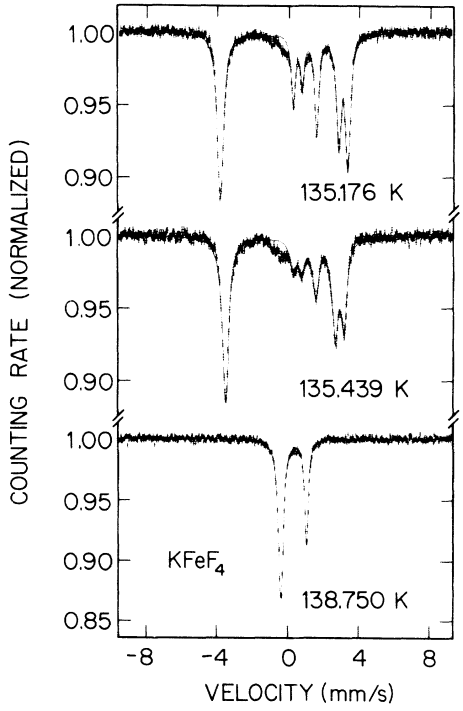

FIG. 4. Mössbauer spectra of single-crystal $KFeF_4$ taken near $T_N = 135.79$ K.

($\eta = 0$) and the γ-ray beam is comparable with the tilting angle $\phi \approx 15°$ of the slightly distorted FeF_6 octahedra.[8,32] Furthermore, the apparent relation $\phi \approx \theta_\gamma \approx \theta$, where θ is the polar angle between V_{zz} and the hyperfine field H, implies that in the ordered state the magnetic moments in both compounds are aligned perpendicular to the layers. This finding is in accordance with previous neutron data[5,6] and can be seen directly in the low-temperature spectra (Fig. 2) where the lines corresponding to $\Delta m = 0$ are almost completely suppressed. The orientation of V_{zz} with respect to the γ-ray direction can also be determined in the paramagnetic phase from the area ratios of the asymmetric quadrupole lines (Figs. 3 and 4). The corresponding values for θ_γ are in agreement with those obtained from the low-temperature spectra (Table IV). Moreover, V_{zz} is negative because the more intense lines ($\Delta m = \pm 1$) are at lower velocities.

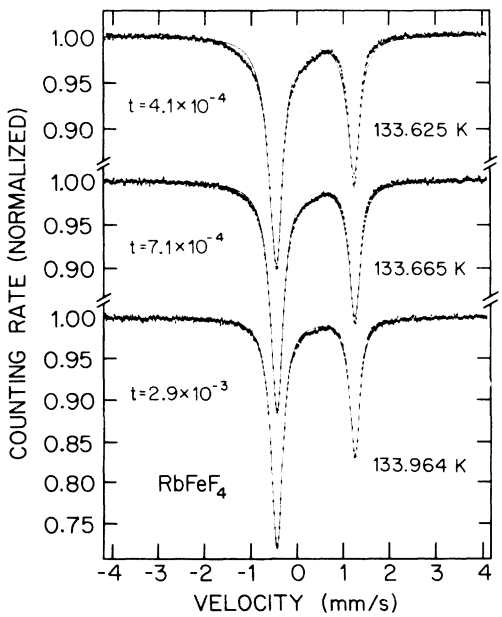

FIG. 3. Mössbauer spectra of single-crystal $RbFeF_4$ taken in the critical region above $T_N = 133.57$ K. The reduced temperature is given as $t = T/T_N - 1$.

The temperature dependence of the reduced hyperfine field $H(T)/H(0)$ is shown in Fig. 5. The extrapolated values for $H(0)$ are 537(4) kG for $RbFeF_4$ and 540(4) kG for $KFeF_4$. These values are typical for trivalent iron ($S = \frac{5}{2}$). In the following we assume that $H(T)$ is proportional to the sublattice magnetization (cf. Sec. II A). Eibschütz *et al.*[7] have shown that for $T/T_N < 0.5$ the hyperfine field $H(T)$ of both compounds is well described by a simple noninteracting spin-wave theory. This model yields rather large values for the zero-point spin deviation $\Delta_0 \simeq 0.16$ (Table III), which is typical for layered antiferromagnets.[1] As shown in Fig. 5 the two reduced sublattice magnetization curves are almost identical for $T/T_N < 0.5$. In the critical region, however, the two curves behave quite differently (see inset in Fig. 5). At the magnetic phase transition a characteristic line broadening $\Delta\Gamma$ due to critical spin fluctuations is observed (critical slowing down). A detailed discussion of the static critical behavior of the order parameter $H(T)/H(0)$ and of the critical spin dynamics above T_N is given in Sec. V.

The temperature dependence of the center shift δ and the quadrupole splitting Δ are represented in Figs. 6 and 7, respectively. The experimental values for δ are typical for

TABLE IV. Summary of various Mössbauer parameters for $RbFeF_4$ and $KFeF_4$ at three typical temperatures. Parameters are defined in the text.

	$RbFeF_4$			$KFeF_4$		
	0 K[a]	90 K	296 K	0 K[a]	90 K	296 K
H (kG)	537(4)	427(2)		540(4)	451(2)	
Δ (mm/s)	−1.70(2)	−1.71(2)	−1.676(2)	−1.47(2)	−1.47(2)	−1.444(3)
δ (mm/s)[b]	0.551(5)	0.545(2)	0.447(2)	0.560(5)	0.557(2)	0.455(2)
η	0.00(5)	0.00(5)		0.00(5)	0.00(5)	
θ (deg)	16(1)	16.7(5)		14(1)	14.1(5)	
θ_γ (deg)	15(1)	15.5(5)	17(2)	11(1)	11.2(5)	13(2)
Γ (mm/s)[c]	0.202(2)	0.203(2)	0.201(2)	0.202(2)	0.204(2)	0.199(2)

[a]Extrapolated values to 0 K.
[b]Relative to α-Fe.
[c]FWHM.

high-spin Fe^{3+}, while the values for Δ are rather large for trivalent fluorides.[7] Note that both quantities δ and Δ display an anomalous behavior near the magnetic transition. Possible reasons for these anomalies are discussed in Sec. V.

V. EXPERIMENTAL CRITICAL BEHAVIOR

A. Static critical exponent β ($T < T_N$)

Under the assumption that the hyperfine field $H(T)$ is proportional to the order parameter $\sigma(T)$ in the critical region, the evaluation of the critical exponent β from hyperfine-field data using Eq. (4) is straightforward (cf. Sec. II A). However, Eq. (4) only leads to reliable values for β if the analysis is based on data taken within the asymptotic critical region (usually defined by $t \lesssim 10^{-2}$).[36] In addition, the critical region depends on the particular magnetic system and thus has to be determined experimentally for each case.[2]

In this work a systematic analysis of the data near T_N was made following the procedure described by Hohenemser and co-workers[2,15]: In this procedure weight-

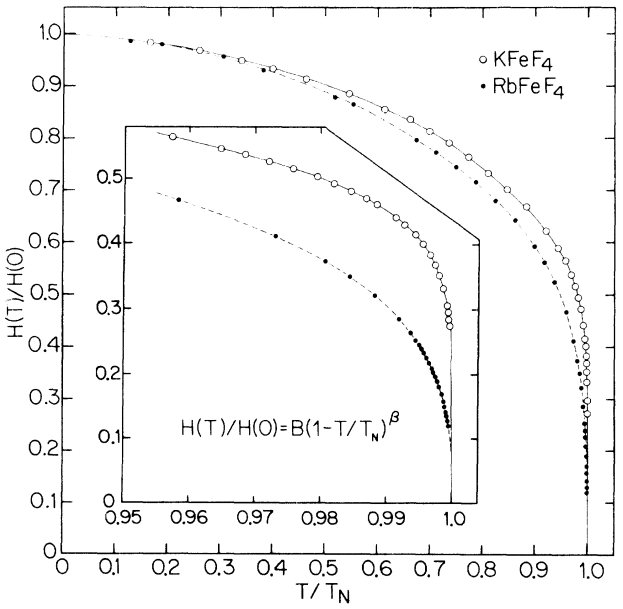

FIG. 5. Reduced hyperfine field $H(T)/H(0)$ as a function of the reduced temperature T/T_N. The critical region is expanded in the inset, where the solid and the dashed lines correspond to fits to the power law given by Eq. (4).

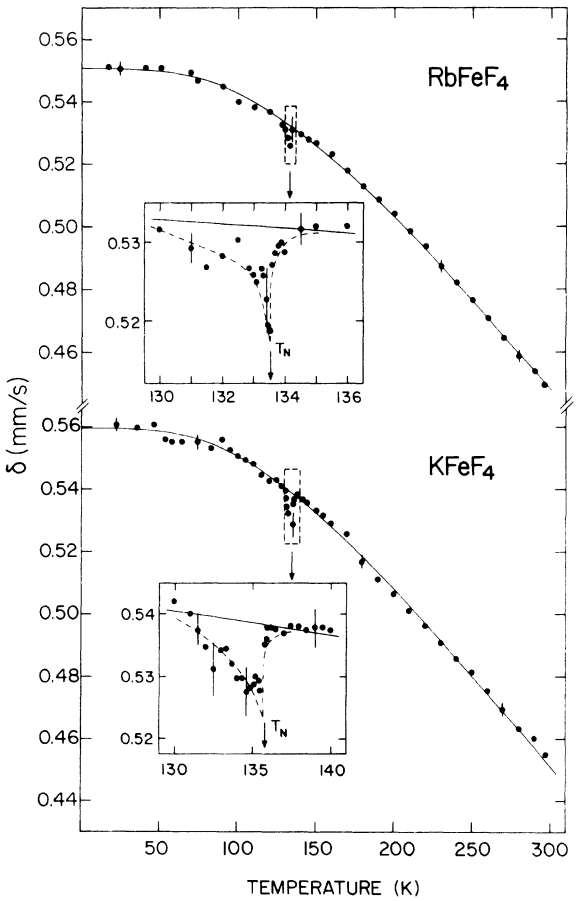

FIG. 6. Center shift δ (relative to metallic iron) as a function of temperature. The solid lines correspond to fits to the Debye model described in the text. An expansion near T_N is given in the inset. The dashed line is meant to guide the eye.

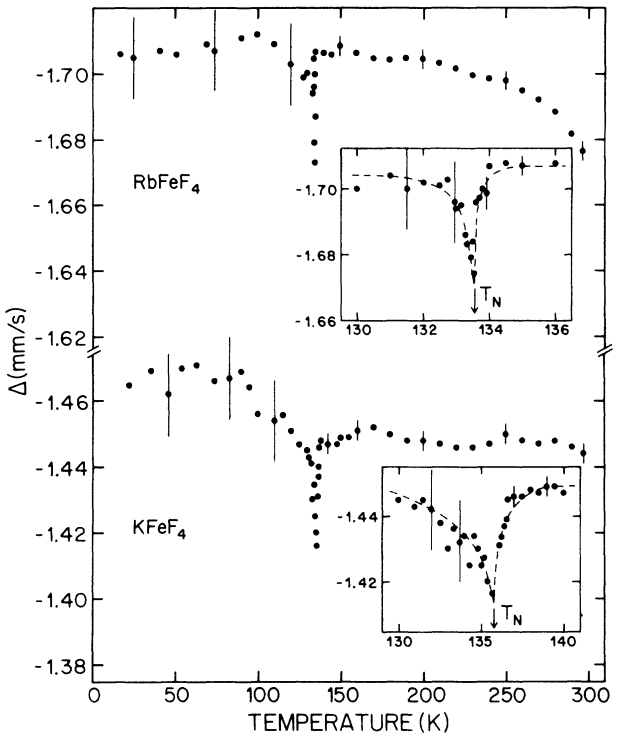

FIG. 7. Quadrupole splitting Δ as a function of temperature. An expansion near T_N is given in the inset. The dashed line is meant to guide the eye.

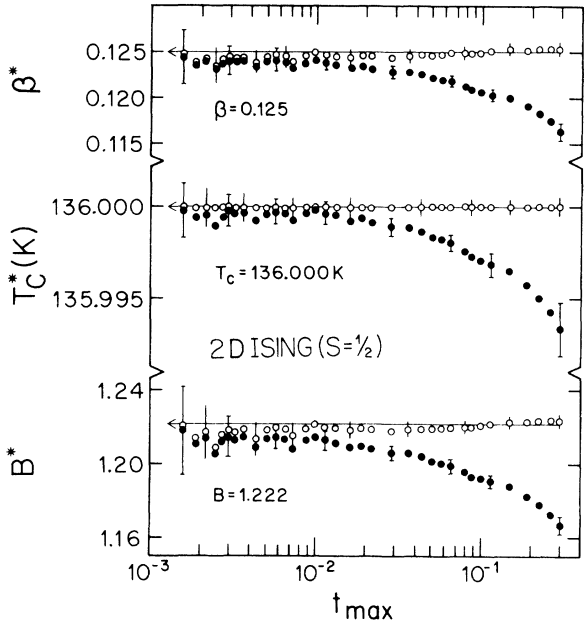

FIG. 8. Variation of critical parameters β^*, T_C^*, and B^* with maximum reduced temperature t_{max} as obtained for computer simulated data for the 2D Ising model (see text). Solid lines refer to the true asymptotic values $\beta=0.125$, $T_C=136$ K, and $B=1.222$. Closed circles correspond to fits to a single power law [Eq. (1)], whereas open circles are obtained from fits to a power law including a correction-to-scaling term [Eq. (2)]. Note the appearance of the asymptotic critical region ($t_{max}\approx 10^{-2}$), where the correction-to-scaling becomes negligibly small.

ed least-squares fits to the power law given by Eq. (4) with the free parameters B, T_N, and β are performed for various temperature regions defined by the maximum reduced temperature t_{max}. Effective values B^*, T_N^*, and β^* are determined as a function of t_{max} by successively omitting data points. This procedure provides an upper limit for the asymptotic critical region where all three quantities B^*, T_N^*, and β^* should remain constant.

The self-consistency of this method was tested on computer-simulated data based on the exact solution of the reduced magnetization $\sigma(T)$ for the 2D Ising model [$S=\frac{1}{2}$ (Ref. 37)]:

$$\sigma(T)=[1-\sinh^{-4}(2J/k_BT)]^{1/8} . \quad (21)$$

Gaussian-distributed errors were generated with a random-number procedure. These errors were comparable to the experimental errors of our data presented in this paper. In order to allow a direct comparison with the experimental data a similar temperature range ($t_{min}=2\times 10^{-4}$) and a comparable density of data points were used for the simulations. The critical temperature was chosen to be $T_C=136$ K. At least ten data points were used in the fitting procedure. The resulting variations of β^*, T_N^*, and B^* as a function of t_{max} are shown in Fig. 8. In the case of a single power law, one can clearly observe the appearance of the asymptotic critical behavior below $t\simeq 10^{-2}$, where all the effective critical parameters remain constant and agree within errors with the universal values. In other words, for temperatures $t<10^{-2}$ a single power law yields reliable results. For $t>10^{-2}$, however, one must consider the correction-to-scaling term given by Eq. (2) in the analysis in order to obtain reasonable values for the critical parameters. Such an analysis for the 2D Ising model with fixed values $\tilde{\Delta}=1$ (Table I) and $A=-0.2255$ is shown in Fig. 8. Indeed, the improvement of the results is remarkable as long as correction-to-scaling is appreciable. In the critical region ($t<10^{-2}$), however, the correction term becomes negligibly small, and the results agree, within errors, with those obtained for the pure power law (Fig. 8). Note that for reduced temperatures $t>0$ effective exponents β^* are obtained that are slightly smaller than the universal $\beta=0.125$ (solid line in Fig. 8). This difference is predicted by Eq. (3) which for the 2D Ising model is given as $\beta^*=\beta-0.2255t+O(t^2)$. The three independent quantities β^*, T_C^*, and B^* are strongly intercorrelated, but in the critical region they all converge to the correct asymptotic values.

The hyperfine-field data for $RbFeF_4$ and $KFeF_4$ were analyzed using the procedure described above. At least thirteen data points were used in the analysis for $RbFeF_4$ and eight for $KFeF_4$. The variation of the effective critical parameters with t_{max} as obtained from the single power law are shown in Figs. 9 and 10 for $RbFeF_4$ and $KFeF_4$, respectively. Note that the critical region for $RbFeF_4$ starts at $t\simeq 10^{-2}$, whereas for $KFeF_4$ the asymptotic region extends up to almost $t=10^{-1}$. The critical parameters as obtained from the flat regions in Figs. 9 and 10 (dashed lines) together with the previous results of other groups are listed in Table V. A log-log plot of the hyperfine-field data, as well as the theoretical prediction

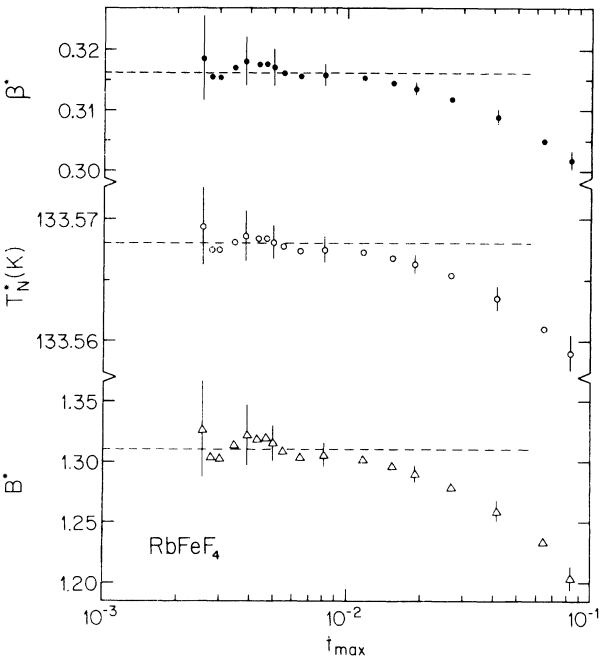

FIG. 9. Variation of the effective critical parameters β^*, T_N^*, and B^* for $RbFeF_4$ with maximum reduced temperature t_{max} as obtained from fits to a single power law [Eq. (4)]. The dashed lines refer to the asymptotic values of $\beta^* \simeq \beta$, $T_N^* \simeq T_N$, and $B^* \simeq B$.

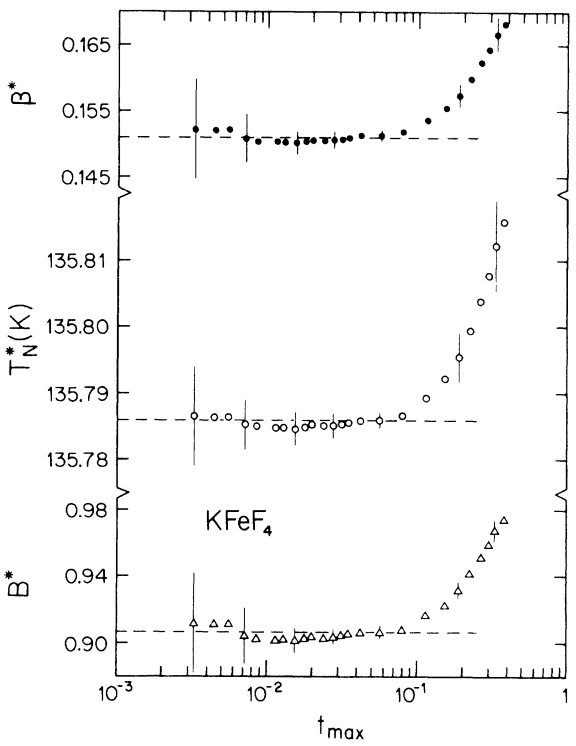

FIG. 10. Variation of the effective critical parameters β^*, T_N^*, and B^* for $KFeF_4$ with maximum reduced temperature t_{max} as obtained from fits to a single power law [Eq. (4)]. The dashed lines refer to the asymptotic values of $\beta^* \simeq \beta$, $T_N^* \simeq T_N$, and $B^* \simeq B$.

for the 2D Ising model ($S = \frac{1}{2}$), are illustrated in Fig. 11. Best fits to the single power law [Eq. (4)] are also shown in the inset of Fig. 5.

The present value $\beta = 0.316(3)$ for $RbFeF_4$ clearly indicates that at temperatures close to T_N $RbFeF_4$ behaves more like a 3D magnetic system ($\beta \simeq \frac{1}{3}$) than a 2D magnetic system ($\beta = \frac{1}{8}$) (Table I). This is because the ratio $|J'/J|$ in Eq. (18) is not sufficiently small to allow 2D magnetic ordering within the layers (cf. Sec. III). $RbFeF_4$ has a small anisotropy parameter, $\alpha \simeq 6.5 \times 10^{-3}$ (Table III), and therefore one would expect a 3D Heisenberg exponent, $\beta = 0.365$ (Table I). The experimental value $\beta = 0.316(3)$, however, is closer to $\beta = 0.325$ predicted for the 3D Ising model (Table I). Note that a quite similar exponent $\beta = 0.316(8)$, $6 \times 10^{-3} < t < 5 \times 10^{-2}$, has been found for the highly isotropic 3D Heisenberg antiferromagnet $RbMnF_3$ ($\alpha \simeq 5 \times 10^{-6}$).[38,1]

For $KFeF_4$, on the other hand, a critical exponent

TABLE V. Static critical parameters for $RbFeF_4$ and $KFeF_4$.

	β	T_N (K)	B	Range of t	Reference
$RbFeF_4$	0.245(5)	133.40(5)	1.18(1)	$10^{-2} < t < 6 \times 10^{-1}$	Eibschütz *et al.*[a]
	0.265(5)	133.8	?	$? < t < 6 \times 10^{-1}$	Rush *et al.*[b]
	0.249(2)	133.08(6)	1.05(5)	$10^{-2} < t < 6 \times 10^{-1}$	This work[c]
	0.316(3)	133.568(5)	1.31(6)	$5 \times 10^{-4} < t < 10^{-2}$	This work[c]
$KFeF_4$	0.182(2)	141.40(2)	1.00	$2 \times 10^{-3} < t < 3.6 \times 10^{-1}$	Heger and Geller[d]
	0.209(8)	141.51(5)	1.12	$2 \times 10^{-3} < t < 4 \times 10^{-2}$	Heger and Geller[d]
	0.185(5)	137.2(1)	0.99(1)	$10^{-2} < t < 2.8 \times 10^{-1}$	Eibschütz *et al.*[e]
	0.185(4)	136.3(1)	1.00(1)	$10^{-2} < t < 2.7 \times 10^{-1}$	This work[f]
	0.161(3)	135.82(2)	0.93(2)	$2.4 \times 10^{-3} < t < 1.2 \times 10^{-1}$	This work[f]
	0.151(3)	135.786(6)	0.91(2)	$3.8 \times 10^{-4} < t < 5.7 \times 10^{-2}$	This work[f]

[a]Reference 4.
[b]Reference 8.
[c]See also Refs. 17 and 35.
[d]Reference 6.
[e]Reference 5.
[f]See also Ref. 35.

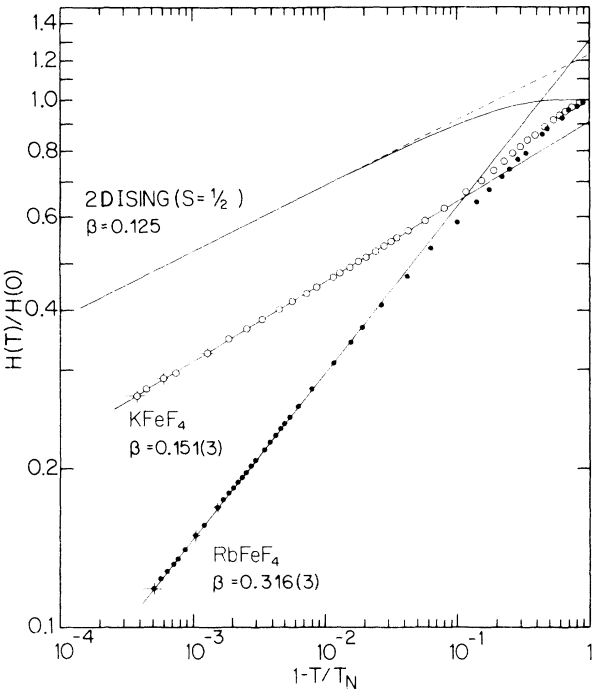

FIG. 11. Plot of the reduced hyperfine field $H(T)/H(0)$ as a function of the reduced temperature $t=1-T/T_N$. The slopes of the straight lines determine the critical exponents $\beta=0.316(3)$ and $\beta=0.151(3)$ for $RbFeF_4$ and $KFeF_4$, respectively. For comparison, the exact solution for the 2D Ising model ($\beta=0.125$) is also shown.

$\beta=0.151(3)$ was found which is close to the exact value $\beta=0.125$ for the 2D Ising model (Table I). Thus, in contrast to $RbFeF_4$, the antiferromagnetic phase transition in $KFeF_4$ is truly 2D in nature as expected from the arguments made in Sec. III. In fact, the experimental β for $KFeF_4$ is similar to those found for other anisotropic 2D Heisenberg antiferromagnets[39] such as K_2NiF_4 [$\beta=0.138(4)$], K_2MnF_4 [$\beta=0.15(1)$], and Rb_2MnF_4 [$\beta=0.16(1)$], or for the 2D XY antiferromagnet $(CH_3NH_3)_2FeCl_4$ [$\beta=0.146(5)$],[40] to give only a few examples.[41]

The discrepancy between the present values for β and the previous values listed in Table V is striking. This is because the latter ones are nonasymptotic values determined outside the appropriate critical region and are therefore inconclusive. Similar results have been reported for various 3D magnetic systems[2] and for the 2D antiferromagnet $(CH_3NH_3)_2FeCl_4$.[40] In general, it is more difficult to measure β for a 2D system where the order parameter near T_C is a much steeper function than for a 3D system (see inset, Fig. 5). Thus great care should be taken in evaluating critical indices in 2D systems. Note that for temperatures outside the critical region the present data yield nonasymptotic values for β that are in agreement with those reported previously (Table V), except for the values of Heger and Geller[6] for $KFeF_4$.

Another point of interest is that all effective critical parameters β^*, T_N^*, and B^* for $KFeF_4$ decrease as t_{max} goes to zero (Fig. 10), in contrast to $RbFeF_4$ (Fig. 9) and the computer simulations for the 2D Ising model (Fig. 8). In addition, the normalization factor $B=0.91(2)$ for $KFeF_4$ is considerably smaller than $B=1.22$ for the 2D Ising model. Values for $B<1$ have been found for a number of "quasi"-2D magnetic systems.[1,40,42] The reason for this unusual behavior of the critical parameters is evident in Fig. 11. At low temperatures, $T/T_N<0.5$, the magnetization curves for $RbFeF_4$ and $KFeF_4$ are very similar (see also Fig. 5). A probable explanation is that at low temperatures the fluctuations of the order parameter are too small to destroy the correlations between the layers, even in the case of $KFeF_4$ where the interlayer coupling J' is much smaller than for $RbFeF_4$ (cf. Sec. III). With increasing temperature, however, the fluctuations become increasingly more important in $KFeF_4$. Finally, close to T_N the 3D correlations are weak enough so that the occurrence of the phase transition is mainly caused by the 2D properties of the system (Fig. 11). This explanation is consistent with the neutron scattering results of Heger and Geller.[6] In other words, the order parameter in $KFeF_4$ shows a crossover from 3D to 2D, in contrast to $RbFeF_4$ which exhibits a 3D critical behavior due to the much stronger coupling between the layers. A similar crossover effect has been observed in the single-layer structure $(CH_3NH_3)_2FeCl_4$,[40] and even more clearly in the double-layer structure $K_3Mn_2F_7$,[42] but no explicit explanation has been given. This crossover phenomenon is most likely the reason for the unusual behavior of the effective critical parameters observed in Fig. 10. Moreover, the fact that for a large number of "quasi"-2D magnetic systems,[1] $KFeF_4$ included, the "critical region" extends up to $t\approx 10^{-1}$ is probably just a consequence of this effect. Note that in contrast to this observation the critical region for the 2D Ising model starts at about $t\simeq 10^{-2}$ (see Fig. 8). However, in order to get a more quantitative picture of this phenomenon, an adequate theory would be needed. To our knowledge there is currently no theory for such an effect.

B. Critical spin fluctuations ($T>T_N$)

Just above T_N a characteristic line broadening $\Delta\Gamma$ of the quadrupole lines due to critical spin fluctuations is observed. Typical Mössbauer spectra of $RbFeF_4$ taken in the critical region above T_N are shown in Fig. 3. The excess linewidth $\Delta\Gamma$ was derived by subtracting Γ_0 from the experimental linewidth Γ [Eq. (14)], where Γ_0 is the average linewidth as obtained from several spectra well above T_N. The values $\Gamma_0=0.201(2)$ mm/s for $RbFeF_4$ and $\Gamma_0=0.197(2)$ mm/s for $KFeF_4$ are comparable to the source linewidth $\Gamma_0=0.198$ mm/s. Near T_N the critical line broadening $\Delta\Gamma$ is well described by the power law given in Eq. (17). The linewidth data of $RbFeF_4$ and $KFeF_4$ were fitted to this power law with D, T_N, and w as free parameters. The corresponding results are summarized in Table VI, and a log-log plot of the data near T_N is shown in Fig. 12. With the use of Eqs. (16) and (17), the excess linewidth is related to the spin auto-correlation time $\tau_c(s)\approx 2\times 10^{-10}\Delta\Gamma$ (mm/s) (see right-hand scale of Fig. 12). The experimental value for the exponent $w=0.81(6)$ in $RbFeF_4$ is somewhat larger than those obtained for

TABLE VI. Dynamic critical parameters for $RbFeF_4$ and $KFeF_4$.

	w	z	$T_N(K)$	D (mm/s)	Range of t
$RbFeF_4$	0.81(6)[a]	2.15(19)[b]	133.577(5)[a]	$(8.3\pm3.2)\times10^{-5}$[a]	$10^{-4}<t<10^{-3}$[a]
$KFeF_4$	0.91(5)[a]	1.34(16)[c]	135.797(6)	$(4.7\pm1.2)\times10^{-5}$	$10^{-4}<t<10^{-3}$
		1.24(6)[d]			

[a]See also Ref. 35.
[b]Equation (13) with $\nu=0.67(5)$.
[c]Equation (13) with $\nu=0.9(1)$.
[d]Equation (13) with $\gamma+2\beta=1.95(5)$.

various 3D Heisenberg ferromagnets [$w\simeq0.6$–0.7 (Ref. 20)] and for the 3D uniaxial antiferromagnet FeF_2 [$w=0.67(2)$].[43] On the other hand, the value $w=0.91(5)$ for $KFeF_4$ is in agreement with $w=0.91(46)$ obtained for the 2D XY antiferromagnet $(CH_3NH_3)_2FeCl_4$; the latter value, however, has a quite large error.[40]

It is of interest to relate the exponent w to the dynamic exponent z. According to Eqs. (12) and (13), this relation involves two static exponents in addition to w. Aside from the present values of β (Table V), to our knowledge no other static exponents have yet been determined.[44] Reliable values for other static exponents such as ν and γ would be desirable. Nevertheless, a quantitative estimation of z is possible. A reasonable value for the critical exponent ν in 3D systems is $\nu=0.67(5)$, based on experimental[1,20] and theoretical work.[14] Experimentally, values of $\nu\simeq0.9$ ($\nu=1$ for 2D Ising model) have been found for various anisotropic 2D Heisenberg antiferromagnets.[39] We therefore assume that $\nu=0.9(1)$ is also a good value for $KFeF_4$. Another experimental fact is that the scaling relation $\gamma+2\beta=2-\alpha=1.95(5)$ holds within error for different 2D magnetic systems.[45] Adopting Eq. (13) and taking the assumptions made above into account, the values of z listed in Table VI are obtained. As expected there is a significant difference between the critical indices z for the two compounds. Thus the critical dynamics also reflect the different nature of the critical behavior of the two magnetic systems. One must compare the experimental values of w and z with those predicted by theory, given in Table II.

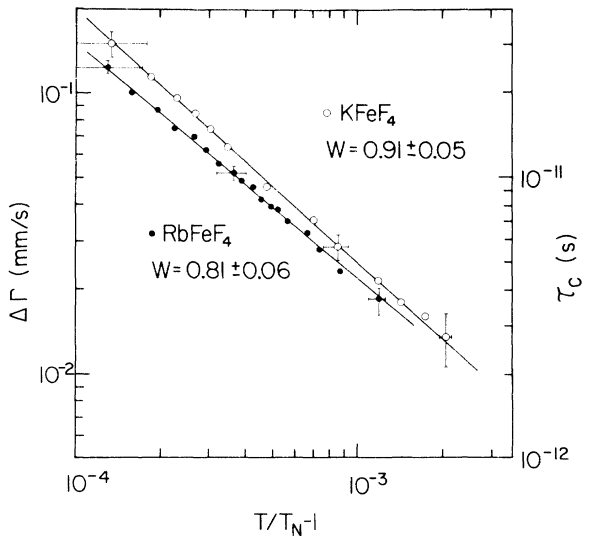

FIG. 12. Plot of the line broadening $\Delta\Gamma$ (FWHM) and corresponding spin-autocorrelation time τ_c (right-hand scale) as a function of the reduced temperature $t=T/T_N-1$ (critical slowing down). The slopes of the straight lines determine the critical exponents $w=0.81(6)$ and $w=0.91(5)$ for $RbFeF_4$ and $KFeF_4$, respectively.

The value of $z=2.15(19)$ for $RbFeF_4$ compares well with $z\simeq2$ predicted for 3D anisotropic antiferromagnets (models A and C), but differs considerably from $z=1.5$ for an isotropic system (model G). This finding is consistent with the Ising-type static exponent $\beta=0.316$ ($d=3$, $n=1$) discussed in Sec. V A. An anisotropic Heisenberg antiferromagnet which belongs to the static universality class ($d=3$, $n=1$) is expected to have the same dynamic critical properties as model C (Ref. 10). Indeed, our experimental values for w and z show best agreement with the theoretical predictions for model C (Tables II and VI). Although the present value of z is only slightly larger than the conventional value $z=2-\eta$, our results seem to indicate a deviation from conventional theory.[10] However, the accuracy of z is insufficient at present to draw definite conclusions.

The two values of z obtained for $KFeF_4$ differ slightly from one another (Table VI). This is because the two results are based on different assumptions for the static exponents. For the following discussion we take the average value $z=1.29(9)$ as a reasonable estimation of z for $KFeF_4$. This value lies between the conventional value $z=1.75$ and $z=1$ predicted for a 2D isotropic antiferromagnet (Table II). A similar value $z=1.21(10)$ was obtained for the 2D Ising-type antiferromagnet Rb_2CoF_4 by means of ultrasonic attenuation studies.[46] However, recent high-resolution inelastic neutron scattering investigations of Rb_2CoF_4 yield $z=1.69(5)$ which is close to the conventional value $z=1.75$ (Table II).[47] The reason for the different values of z is not clear. One should note, however, that in contrast to the neutron measurements, crucial assumptions were made to deduce z from the ultrasonic data.[46,47] Recently, Mazenko and Valls[21] have pointed out that all the current theoretical methods for determining z for model A [$n=1$, $d=2$ (Ref. 10)] are inconclusive, although a particular model gives reliable static exponents. As a consequence, the values of z available in the literature[21] vary over a wide range between 1.4 and

2.2 (Table II). According to these authors, this discrepancy seems to be associated with the existence of a dynamic critical region much narrower than the static critical region. An evaluation of z in this narrow dynamic critical region is problematic, but outside the asymptotic region one expects dynamic scaling with a conventional value of z.[21] Here the question arises: Is there a "crossover" in the exponent w (and corresponding z) for $KFeF_4$ as T goes to T_N? A detailed investigation of this question is in progress. In addition, it is interesting to note that a quite similar value of $z=1.22(47)$ is also obtained for the 2D planar antiferromagnet $(CH_3NH_3)_2FeCl_4$ with $w=0.91(46)$, $\beta=0.146(5)$, and $\gamma=1.67(3)$.[40,45] Further experimental and theoretical work is still required to get a deeper understanding on critical dynamics in 2D magnetic systems.

C. Center shift and quadrupole splitting

The temperature dependence of the center shift δ is shown in Fig. 6. At the magnetic phase transition a noticeable anomaly in δ is observed for both compounds. A quite similar observation has been reported previously for $KFeF_4$ by Heger and Geller,[6] but no explanation has been given.

The center shift δ is a sum of two different contributions:

$$\delta(T)=\delta_{IS}(T)+\delta_{SOD}(T) . \tag{22}$$

The isomer shift δ_{IS} is proportional to the difference of the total electron charge density at the Mössbauer nucleus between source and absorber and is in general only weakly temperature dependent. A weak temperature dependence of δ_{IS} may arise through the effect of thermal expansion on the electron density at the nucleus.[48] At a magnetic phase transition, however, δ_{IS} may change considerably when the transition is associated with a rearrangement of the electron charge distribution.[49] The second-order Doppler shift δ_{SOD}, on the other hand, is a relativistic effect that is due to the thermal motion of the Mössbauer nucleus in the lattice. In the Debye model approximation δ_{SOD} (in velocity units) is simply given by[48]

$$\delta_{SOD}(T)=-(9k_B\Theta_D/16mc)\left[1+8(T/\Theta_D)^4\int_0^{\Theta_D/T}x^3(e^x-1)^{-1}dx\right] . \tag{23}$$

According to the theory of Bashkirov and Selyutin,[50] the Debye temperature Θ_D of a magnetically ordered solid depends on the state of magnetization,

$$\Theta_D(T)=\Theta_D^0[1+B_0\sigma^2(T)]^{1/2} , \quad 0\le B_0\le 1 \tag{24}$$

where Θ_D^0 is the paramagnetic Debye temperature, B_0 is a numerical coefficient, and $\sigma(T)$ is the reduced (sublattice) magnetization. In the critical region just below T_N one may write for Θ_D [cf. Eq. (1)]

$$\Theta_D(t)\underset{t\to 0}{=}\Theta_D^0(1+C_0t^{2\beta})^{1/2} , \quad 0\le C_0\lesssim 2.5 \tag{25}$$

where C_0 is a numerical constant, $t=1-T/T_N$ is the reduced temperature, and β is the critical exponent of the order parameter. Thus at T_N the thermal shift δ_{SOD} may display an anomalous behavior which according to Eq. (25) should in principle be more pronounced for a 2D magnetic system ($\beta=\frac{1}{8}$) than for a 3D magnetic system ($\beta\simeq\frac{1}{3}$). Whether such an anomaly is observable or not depends crucially on the ratio Θ_D/T_N. In the high-temperature limit ($T_N>\Theta_D$) δ_{SOD} is almost independent of Θ_D, and therefore the effect is in general too small to be measured. This has been confirmed in the case of metallic iron ($\Theta_D/T_C\simeq 0.4$).[51] For $T_N<\Theta_D$, however, the effect is observable, because in this temperature region δ_{SOD} is very sensitive to Θ_D. Experimentally, a weak indication of this effect has been found in FeF_3 ($\Theta_D/T_N\simeq 1.4$).[48] To illustrate this effect, a theoretical calculation of δ_{SOD} based on Eqs. (23) and (24) for $\Theta_D^0=450$ K and $T_N=135$ K is represented in Fig. 13. For comparison the 2D Ising model ($S=\frac{1}{2}$) and the mean-field approximation (MFA) ($S=\frac{5}{2}$) were used for the reduced sublattice magnetization $\sigma(T)$. Note that for the 2D Ising model there is a remarkable anomaly in δ_{SOD} at T_N, even for $B_0=0.1$, while for the MFA model only a kink in δ_{SOD} is observed. This is due to fact that close to the transition temperature Θ_D varies more rapidly for the 2D Ising model ($\beta=\frac{1}{8}$) than for the mean-field approximation ($\beta=\frac{1}{2}$) as shown in Fig. 13. In an experiment one measures the total energy shift δ, and in most cases a separation of δ_{IS} and δ_{SOD} is difficult. That means an anomaly in δ implies either a change in δ_{IS} or in δ_{SOD}, or even a combination of both. Assuming that the effect is only due to δ_{SOD}, and that δ_{IS} is temperature independent, one may try to use the magnetization-dependent Debye model to describe this

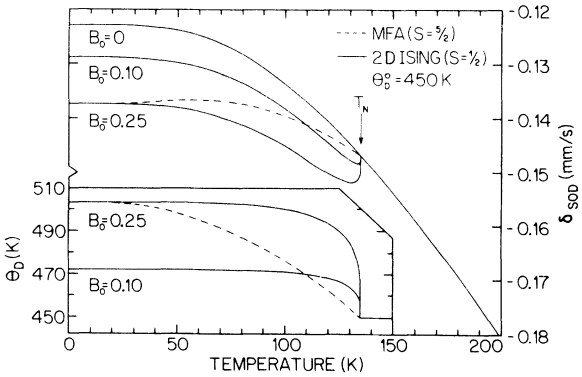

FIG. 13. Theoretical calculation of the thermal shift δ_{SOD}, based on the magnetization-dependent Debye model described in the text. The calculations were made for $T_N=135$ K, $\Theta_D^0=450$ K and different values of B_0. For the reduced sublattice magnetization the 2D Ising model (solid lines) and the mean-field approximation (dashed line) were used. The corresponding temperature variations of the Debye temperature Θ_D are shown in the inset.

phenomenon. However, an attempt to fit the experimental data with this simple model failed. The best fits (excluding data points near T_N) were obtained for $B_0=0$ and $\Theta_D^0=495(50)$ K for $RbFeF_4$ and $\Theta_D^0=470(50)$ K for $KFeF_4$ (solid curves in Fig. 6). Therefore, we may conclude that the magnetization-dependent Debye model is insufficient to explain the critical anomaly in δ.

It is known that in magnetic systems with strong magnon-phonon coupling critical spin fluctuations below T_C may considerably affect the phonon spectrum.[52] As a consequence a softening of the phonon spectrum at T_C occurs which may have an influence on the recoil-free fraction f and the thermal shift δ_{SOD}.[53] In the magnetostrictive ferromagnet $DyFe_2$ Shechter *et al.*[53] have observed large dips in the f factor and the center shift δ near T_C, probably arising from this effect. Some evidence for such a phenomenon is also found in the present work, although the effect is much smaller. The onset of the anomalous behavior in δ (Fig. 6) appears to be associated with the observed line broadening due to critical fluctuations below T_N, indicating a correlation between these two phenomena. On the other hand, the anomaly in δ could be due as well to a magnetically induced change in the isomer shift δ_{IS} as mentioned above.

The temperature dependence of the quadrupole splitting Δ is represented in Fig. 7. Note that Δ for $KFeF_4$ in the ordered phase is slightly larger than in the paramagnetic state, in contrast to $RbFeF_4$ where Δ remains constant through the magnetic transition within experimental error (anomalous behavior near T_N excluded). The small discontinuity in Δ observed in $KFeF_4$ is probably induced magnetically. In addition to the anomaly in the center shift δ, the quadrupole splitting Δ shows a quite similar irregular behavior near T_N as indicated in Fig. 7. Moreover, the overlap of the temperature regions where the anomalies in δ and Δ occur suggests that both effects are correlated (see Figs. 6 and 7). These anomalies are obviously related to the magnetic ordering and are most likely induced by the critical fluctuations. The true mechanism of these phenomena, however, is not understood yet. Further experiments like ultrasonic attenuation studies, neutron scattering experiments, and precise measurements of the recoil-free fraction would be required to test this interpretation.

VI. CONCLUSIONS

We have used the Mössbauer technique to study the static and dynamic critical behavior of the layered antiferromagnets $RbFeF_4$ and $KFeF_4$. The main results can be summarized as follows.

Both $RbFeF_4$ and $KFeF_4$ show a second-order phase transition at $T_N=133.57(2)$ K and $T_N=135.79(2)$ K, respectively. Special attention was paid to a careful evaluation of the critical exponent β of the order parameter by determining the appropriate asymptotic critical region. The self-consistency of our method was tested on computer-simulated data based on the 2D Ising model. The asymptotic values of β as obtained from a single power law are $\beta=0.316(3)$ for $RbFeF_4$ and $\beta=0.151(3)$ for $KFeF_4$, indicating that $RbFeF_4$ shows a 3D critical behavior, whereas in $KFeF_4$ the transition is essentially 2D in character. This result is consistent with the fact that in $KFeF_4$ the coupling between adjacent layers is canceled due to symmetry arguments leading to a much weaker interlayer coupling than in $RbFeF_4$. In addition, the experimental transition temperature T_N of $KFeF_4$ compares well with the Stanley-Kaplan temperature T_{SK} ($T_N/T_{SK}\simeq 1.03$). Below T_N, both systems are ordered in three dimensions because of the residual interaction between the layers. When approaching T_N, however, the 3D correlations in $KFeF_4$ become sufficiently weak so that the phase transition is mainly governed by the 2D properties of the system. Similar crossover effects have also been observed in the single-layer structure $(CH_3NH_3)_2FeCl_4$ (Refs. 40 and 45) and in the double-layer structure $K_3Mn_2F_7$.[42] The present values of β differ considerably from those found by other groups.[4–8] This is because the latter values were determined outside the asymptotic critical region. For temperatures not sufficiently close to T_N our data yield similar nonasymptotic results.

Just above T_N a characteristic line broadening $\Delta\Gamma$ due to critical fluctuations is observed. According to the idealized relaxation theory of Bradford and Marshall,[22] $\Delta\Gamma$ is proportional to the spin-autocorrelation time τ_c which at T_N diverges with a critical exponent w (critical slowing down). We find that $w=0.81(6)$ for $RbFeF_4$ and $w=0.91(5)$ for $KFeF_4$. From these values we have estimated values for the dynamic critical exponent z using the static scaling relations. The present value $z=2.15(19)$ for $RbFeF_4$ compares well with $z=2.17$ predicted by dynamic scaling theory for a 3D anisotropic antiferromagnet [model C (Ref. 10)] and seems to indicate a deviation from the conventional value $z=2-\eta$. This result is also compatible with the Ising-type static exponent $\beta=0.316(3)$. For the 2D system $KFeF_4$ a value $z=1.29(9)$ is found, which is significantly smaller than the conventional value $z=1.75$. A similar nonconventional value $z=1.21(10)$ has been reported for the 2D Ising-type antiferromagnet Rb_2CoF_4.[46] However, a theoretical interpretation of our experimental results is difficult at present, since current theory does not provide a reliable value of z for the dynamic universality class ($n=1$, $d=2$).[21] More theoretical and experimental work must be done in order to get a better insight into critical dynamics in 2D magnetic systems. To further improve the present values of z, precise measurements of static exponents other than β or even a direct measurement of z would be required. In addition, it would be more appropriate to make use of a relaxation theory of the Mössbauer line shape which takes into account anisotropic spin fluctuations, most likely present in such weakly anisotropic Heisenberg systems near T_c.[39,42,43,47]

The values for T_N as deduced from best fits to the power laws defined by Eqs. (4) and (17) agree within error with the experimental values $T_N=133.58(2)$ for $RbFeF_4$ and $T_N=135.80(2)$ for $KFeF_4$ as obtained from the characteristic peak of the linewidth (cf. Tables V and VI). This result further supports the self-consistency of the data analysis applied in this work.

The center shift δ and quadrupole splitting Δ display an

anomalous behavior at T_N that appears to be associated with the onset of magnetic ordering. The magnetization-dependent Debye model[50] does not explain the anomaly in the center shift δ. Whether the anomalous behavior of δ is due to the isomer shift or due to the second-order Doppler shift, or even due to a combination of both, remains unclear. The mechanism responsible for the pronounced dips in the quadrupole splitting Δ observed at T_N is also not yet understood. However, the anomalies in δ and Δ appear to be correlated with the critical line broadening below T_N and are therefore most likely induced by the critical fluctuations.

It is hoped that our results will encourage experimentalists to do supplementary measurements on the critical behavior of these interesting magnetic systems with other techniques. Detailed neutron scattering studies would especially be desirable.

ACKNOWLEDGMENTS

We are grateful to Dr. B. M. Wanklyn (Oxford University) and to Dr. M. Eibschütz (Bell Laboratories) for kindly providing us with the single crystals. Also, we wish to thank Professor W. Kündig, Professor P. F. Meier, and Professor S. Milošević for helpful discussions and comments and to Dr. R. F. Kiefl and Dr. B. D. Patterson for assistance in manuscript preparation. Support by the Swiss National Science Foundation is gratefully acknowledged.

---

*Permanent address: Faculty of Natural and Mathematical Sciences, Department of Physics, 11000 Belgrade, Yugoslavia.

[1]For a review of early work, see L. J. de Jongh and A. R. Miedema, Adv. Phys. 23, 1 (1974).

[2]R. M. Suter and C. Hohenemser, J. Appl. Phys. 50, 1814 (1979).

[3]M. A. Kobeissi, Phys. Rev. B 24, 2380 (1981).

[4]M. Eibschütz, H. J. Guggenheim, and L. Holmes, J. Appl. Phys. 42, 1485 (1971).

[5]M. Eibschütz, G. R. Davidson, H. J. Guggenheim, and D. E. Cox, in *Magnetism and Magnetic Materials—1971 (Chicago)*, Proceedings of the 17th Annual Conference on Magnetism and Magnetic Materials, edited by C. D. Graham and J. J. Rhyne (AIP, New York, 1972), p. 670.

[6]G. Heger and R. Geller, Phys. Status Solidi B 53, 227 (1972).

[7]M. Eibschütz, G. R. Davidson, and H. J. Guggenheim, Phys. Rev. B 9, 3885 (1974).

[8]J. D. Rush, A. Simopoulos, M. F. Thomas, and B. M. Wanklyn, Solid State Commun. 18, 1039 (1976).

[9]See, e.g., S.-k. Ma, *Modern Theory of Critical Phenomena* (Benjamin, New York, 1976).

[10]P. C. Hohenberg and B. I. Halperin, Rev. Mod. Phys. 49, 435 (1977); Phys. Rev. 177, 952 (1969); B. I. Halperin, P. C. Hohenberg, and S.-k. Ma, Phys. Rev. B 10, 139 (1974).

[11]G. Ahlers, in *Quantum Liquids*, edited by J. Ruvalds and T. Regge (North-Holland, New York, 1978), p. 1.

[12]A. Aharony and G. Ahlers, Phys. Rev. Lett. 44, 782 (1980).

[13]M. C. Chang and A. Houghton, Phys. Rev. Lett. 44, 785 (1980).

[14]J. C. Le Guillou and J. Zinn-Justin, Phys. Rev. Lett. 39, 95 (1977).

[15]C. Hohenemser, in *Proceedings of the International Conference on Mössbauer Spectroscopy*, edited by A. Z. Hrynkiewicz and J. A. Sawicki (Akademia Górniczo-Hutnicza im. S. Staszica, Kracow, 1975), Vol. 2, pp. 239–256.

[16]C. Hohenemser, T. Kachnowski, and T. K. Bergstresser, Phys. Rev. B 13, 3154 (1976).

[17]I. M. Savić, H. Keller, W. Kündig, and P. F. Meier, Phys. Lett. 83A, 471 (1981).

[18]C. Hohenemser, R. M. Suter, L. Chow, M. A. Kobeissi, R. Dunlap, and A. M. Gottlieb, Hyperfine Interact. 10, 887 (1981).

[19]C. Hohenemser, L. Chow, and R. M. Suter, Phys. Rev. B 26, 5056 (1982).

[20]R. M. Suter and C. Hohenemser, Phys. Rev. Lett. 41, 705 (1978).

[21]G. F. Mazenko and O. T. Valls, Phys. Rev. B 24, 1419 (1981), and references therein.

[22]E. Bradford and W. Marshall, Proc. Phys. Soc. London 87, 731 (1966).

[23]M. A. Kobeissi, R. Suter, A. M. Gottlieb, and C. Hohenemser, Phys. Rev. B 11, 2455 (1975), and Ref. 8 therein.

[24]L. L. Liu and H. E. Stanley, Phys. Rev. B 8, 2279 (1973).

[25]N. D. Mermin and H. Wagner, Phys. Rev. Lett. 17, 1133 (1966).

[26]H. E. Stanley and T. A. Kaplan, Phys. Rev. Lett. 17, 913 (1966).

[27]M. E. Lines, J. Appl. Phys. 40, 1352 (1969).

[28]K. Binder and D. P. Landau, Phys. Rev. B 13, 1140 (1976).

[29]D. Babel, Z. Naturforsch. 23a, 1417 (1968).

[30]A. Tressaud, J. Galy, and J. Portier, Bull. Soc. Fr. Mineral. Crystallogr. 92, 335 (1969).

[31]A. Tressaud, J. Portier, R. de Pape, and P. Hagenmuller, J. Solid State Chem. 2, 269 (1970).

[32]G. Heger, R. Geller, and D. Babel, Solid State Commun. 9, 335 (1971).

[33]W. Kündig, A. B. Denison, and P. Rüegsegger, Phys. Lett. 42A, 199 (1972).

[34]W. Hofmann, H. Keller, and W. Kündig, Nucl. Instrum. Methods 143, 609 (1977), and references therein.

[35]I. M. Savić and H. Keller, Helv. Phys. Acta 54, 234 (1981); 54, 603 (1981).

[36]R. F. Wielinga, in *Progress in Low Temperature Physics*, edited by C. J. Gorter (North-Holland, Amsterdam, 1970), Vol. VI, Chap. 8, pp. 333–373.

[37]M. E. Fisher, Rep. Prog. Phys. 30, 615 (1967).

[38]L. M. Corliss, A. Delapalme, J. M. Hastings, H. Y. Lau, and R. Nathans, J. Appl. Phys. 40, 1278 (1969).

[39]R. J. Birgeneau, J. Als-Nielsen, and G. Shirane, Phys. Rev. B 16, 280 (1977), and Refs. 2 and 6 therein.

[40]H. Keller, W. Kündig, and H. Arend, J. Phys. (Paris) Colloq. 37, C6-629 (1976); Physica 86-88B, 683 (1977).

[41]For more examples see, e.g., Ref. 1.

[42]C. M. J. van Uijen, E. Frikkee, and H. W. de Wijn, Phys. Rev. B 19, 509 (1979).

[43]A. M. Gottlieb and P. Heller, Phys. Rev. B 3, 3615 (1971).

[44]The mean-field-like value $\nu=0.60$ for $KFeF_4$ given in Ref. 6 seems to be questionable. See Ref. 39 for an explanation.

[45]H. Keller, Ph.D. thesis, University of Zürich, 1977 (unpublished).

[46]M. Suzuki, K. Kato, and H. Ikeda, J. Phys. Soc. Jpn. 49, 514 (1980).

[47]M. T. Hutchings, H. Ikeda, and E. Janke, Phys. Rev. Lett. 49, 386 (1982). Note that a similar value $z=1.67(13)$ is also obtained from the exponent $w=\nu(z-\eta)=1.46(7)$ first measured by C. Bucci, G. Guidi, and C. Vignali [Solid State Commun. 10, 803 (1972)] using NMR (see also Table II).

[48]G. K. Wertheim, D. N. E. Buchanan, and H. J. Guggenheim, Phys. Rev. B 2, 1392 (1970).

[49]R. S. Preston, in *Mössbauer Isomer Shifts,* edited by G. K. Shenoy and F. E. Wagner (North-Holland, Amsterdam, 1978), p. 281.

[50]Sh. Sh. Bashkirov and G. Ya. Selyutin, Phys. Status Solidi 26, 253 (1968).

[51]M. A. Kobeissi, L. Chow, and C. Hohenemser, Hyperfine Interact. 4, 485 (1978).

[52]M. Tachiki, S. Maekawa, R. Treder, and M. Levy, Phys. Rev. Lett. 34, 1579 (1975).

[53]H. Shechter, D. Bukshpan-Ash, and I. Nowik, Phys. Rev. B 14, 3087 (1976).